

Nonsymmorphic Weyl superconductivity in UPt_3 based on E_{2u} representation

Youichi Yanase*

Department of Physics, Graduate School of Science, Kyoto University, Kyoto 606-8502, Japan

(Received 23 February 2016; revised manuscript received 8 September 2016; published 7 November 2016)

We show that a heavy fermion superconductor UPt_3 is a topological Weyl superconductor with tunable Weyl nodes. Adopting a generic order parameter in the E_{2u} representation allowed by nonsymmorphic crystal symmetry, we clarify unusual gap structure and associated topological properties. The pair creation, pair annihilation, and coalescence of Weyl nodes are demonstrated in the time-reversal symmetry broken B-phase. At most 98 point nodes compatible with Blount's theorem give rise to line-node-like behaviors in low-energy excitations, consistent with experimental results. We also show an *arc* node protected by the nonsymmorphic crystal symmetry on the Brillouin zone face, which is a counterexample of Blount's theorem.

DOI: [10.1103/PhysRevB.94.174502](https://doi.org/10.1103/PhysRevB.94.174502)

Superconductivity with nontrivial symmetry and topology is attracting renewed interest stimulated by enormous studies of topological insulators and superconductors [1–4]. Strongly correlated electron systems are the platform of such unconventional superconductivity [5]. A heavy fermion superconductor UPt_3 discovered in the 1980s [6] unambiguously exhibits exotic properties, that is, multiple superconducting phases in the field-temperature plane [Fig. 1(a)] [7–9]. The presence of the multiple superconducting phases is a direct evidence for a multicomponent non-*s*-wave order parameter [10]. Comparison between experiments and theories points to odd-parity spin-triplet superconductivity [11–13]. Because odd-parity superconductivity is often accompanied by topological order [2,14–16], it may be interesting to clarify the topological properties of UPt_3 .

Topological order in superconductors is closely related to the symmetry and nodal structure of superconductivity. Despite intensive studies for three decades, the symmetry of superconductivity in UPt_3 is still under debate. However, a chiral *f*-wave state with orbital angular momentum $L_z = \pm 2$ [11] allowed in hexagonal crystals [see Fig. 1(b)] is supported by nodal excitations [12] and broken time-reversal symmetry [17] as well as by a phase sensitive measurement [18]. On the other hand, a recent thermal conductivity measurement points to another *f*-wave state with $L_z = \pm 1$ [19].

In spite of these intensive studies, the *f*-wave pairing states are incompatible with Blount's theorem [20,21] which proves the absence of line node in odd-parity superconductors [22]. Although line node behaviors have been observed in UPt_3 [12], Blount's theorem implies that line nodes are fragile against perturbation preserving the symmetry of the system. Indeed, the line nodes disappear as a result of the mixing of *f*-wave Cooper pairs with *p*-wave ones in the same irreducible representation. According to the symmetry classification [10], not only the chiral *f*-wave state with $L_z = \pm 2$ [11] but also a *p*-wave state (and the *f*-wave state with $L_z = \pm 1$ [19]) belong to the E_{2u} representation of D_{6h} point group. Therefore, a generic E_{2u} state is induced by a mixed (*p* + *f*)-wave Cooper pairing. In this paper we clarify the nodal gap structure and specify the topological properties of a generic E_{2u} state in UPt_3 . It is revealed that the B-phase is a Weyl superconducting

state [23] analogous to Weyl semimetals [24–26] discovered recently [27–30]. We furthermore demonstrate pair creation, pair annihilation, and coalescence of Weyl nodes which do not occur in other chiral Weyl superconductors [31–34].

Our study is based on a Bogoliubov–de Gennes (BdG) Hamiltonian,

$$\begin{aligned} \mathcal{H}_{\text{BdG}} = & \sum_{k,m,s} \xi(\mathbf{k}) c_{kms}^\dagger c_{kms} + \sum_{k,s} [a(\mathbf{k}) c_{k1s}^\dagger c_{k2s} + \text{H.c.}] \\ & + \sum_{k,m,s,s'} \alpha_m \mathbf{g}(\mathbf{k}) \cdot \mathbf{s}_{ss'} c_{kms}^\dagger c_{kms'} \\ & + \frac{1}{2} \sum_{k,m,m',s,s'} [\Delta_{mm's's'}(\mathbf{k}) c_{kms}^\dagger c_{-km's'}^\dagger + \text{H.c.}], \quad (1) \end{aligned}$$

where \mathbf{k} , $m = 1, 2$, and $s = \uparrow, \downarrow$ are momentum, sublattice, and spin, respectively. Based on the crystal structure of UPt_3 illustrated in Fig. 1(b), we adopt an intrasublattice kinetic energy, $\xi(\mathbf{k}) = 2t \sum_{i=1,2,3} \cos \mathbf{k}_\parallel \cdot \mathbf{e}_i + 2t_z \cos k_z - \mu$, and intersublattice hopping term, $a(\mathbf{k}) = 2t' \cos \frac{k_z}{2} \sum_{i=1,2,3} e^{i\mathbf{k}_\parallel \cdot \mathbf{r}_i}$, with $\mathbf{k}_\parallel = (k_x, k_y)$ and $\mathbf{e}_1 = (1, 0)$, $\mathbf{e}_2 = (-\frac{1}{2}, \frac{\sqrt{3}}{2})$, $\mathbf{e}_3 = (-\frac{1}{2}, -\frac{\sqrt{3}}{2})$, $\mathbf{r}_1 = (\frac{1}{2}, \frac{1}{2\sqrt{3}})$, $\mathbf{r}_2 = (-\frac{1}{2}, \frac{1}{2\sqrt{3}})$, and $\mathbf{r}_3 = (0, -\frac{1}{\sqrt{3}})$. Since D_{3h} local symmetry at uranium ions lacks inversion symmetry, Kane-Mele spin-orbit coupling (SOC) with $\mathbf{g}(\mathbf{k}) = \hat{z} \sum_{i=1,2,3} \sin \mathbf{k}_\parallel \cdot \mathbf{e}_i$ [35] appears in a sublattice-dependent way. The coupling constant is $(\alpha_1, \alpha_2) = (\alpha, -\alpha)$ so as to preserve the global D_{6h} symmetry [1,36,37]. The intersublattice SOC is prohibited because the intersublattice bonds respect the inversion symmetry.

Quantum oscillation measurements combined with band structure calculations [12,38–41] have shown a pair of FSs centered at the *A*-point (*A*-FSs), three FSs at the Γ point (Γ -FSs), and two FSs at the *K* point in UPt_3 . Since small FSs enclosing the *K* point give a small density of states (DOS), they may play a minor role. Therefore, we study the superconducting properties of *A*-FSs and Γ -FSs one by one. By choosing a parameter set $(t, t_z, t', \alpha, \mu) = (1, -4, 1, 2, 12)$ our two band model reproduces a pair of *A*-FSs, while another set $(t, t_z, t', \alpha, \mu) = (1, 4, 1, 0, 16)$ reproduces the topology of Γ -FS. Since the SOC is negligible for the Γ -FS, we simply set $\alpha = 0$ in the latter parameter set.

Order parameter of the E_{2u} state is generally represented by $\hat{\Delta}(\mathbf{k}) = \eta_1 \hat{\Gamma}_1 + \eta_2 \hat{\Gamma}_2$ with basis functions $\hat{\Gamma}_1$ and $\hat{\Gamma}_2$

*yanase@scphys.kyoto-u.ac.jp

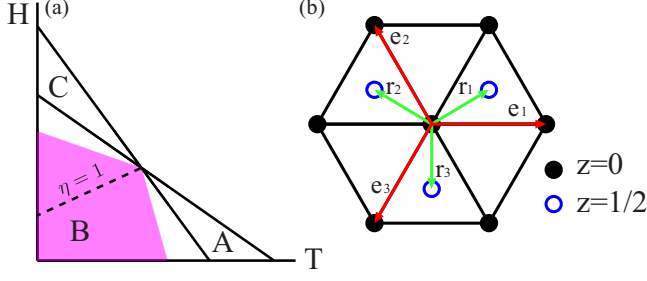


FIG. 1. (a) Multiple superconducting phases in UPt_3 . Shaded region shows the Weyl superconducting phase. (b) Crystal structure of UPt_3 . Uranium ions form AB-stacked triangular lattice. Two-dimensional vectors, \mathbf{e}_i and \mathbf{r}_i , are shown by arrows.

composed of several components. Although the purely f -wave state has been intensively investigated [11], an admixture of a p -wave component is allowed by symmetry. Besides these components, a sublattice-singlet spin-triplet d -wave component naturally accompanies the f -wave component because of the nonsymmorphic crystal structure of UPt_3 [42]. Taking into account all the components, we study the E_{2u} state with

$$\hat{\Gamma}_1 = [\delta\{p_x(\mathbf{k})s_x - p_y(\mathbf{k})s_y\}\sigma_0 + f_{(x^2-y^2)z}(\mathbf{k})s_z\sigma_x - d_{yz}(\mathbf{k})s_z\sigma_y]is_y, \quad (2)$$

$$\hat{\Gamma}_2 = [\delta\{p_y(\mathbf{k})s_x + p_x(\mathbf{k})s_y\}\sigma_0 + f_{xyz}(\mathbf{k})s_z\sigma_x - d_{xz}(\mathbf{k})s_z\sigma_y]is_y, \quad (3)$$

where s_α and σ_α are Pauli matrix in the spin and sublattice space, respectively. The orbital functions, $p_i(\mathbf{k})$, $d_i(\mathbf{k})$, and $f_i(\mathbf{k})$, are obtained by assuming short-range Cooper pairs on neighboring \mathbf{r}_i and \mathbf{e}_i bonds [42]. This choice is consistent with empirical rules obtained by microscopic calculations for many unconventional superconductors [5]. We choose $|\delta| \ll 1$ to study a dominantly f -wave state. Two-component order parameters are parametrized as $(\eta_1, \eta_2) = \Delta(1, i\eta)/\sqrt{1+\eta^2}$ by a real parameter η . Ratio of η_1 and η_2 is pure-imaginary since the condensation energy is maximally gained in the chiral superconducting state. Thus the B-phase is a chiral state, where the range of η is $0 < \eta < \infty$ [43]. It is believed that a weak breakdown of hexagonal symmetry stabilizes the A- and C-phases [11, 12, 43–45]. We assume that the A-phase is the Γ_2 state ($\eta = \infty$), while the C-phase is the Γ_1 state ($\eta = 0$).

The BdG Hamiltonian is represented in the Nambu space $\mathcal{H}_{\text{BdG}} = \frac{1}{2} \sum_{\mathbf{k}} \hat{c}_{\mathbf{k}}^\dagger \hat{H}_{\text{BdG}}(\mathbf{k}) \hat{c}_{\mathbf{k}}$, with $\hat{c}_{\mathbf{k}} = (c_{k1\uparrow}, c_{k2\uparrow}, c_{k1\downarrow}, c_{k2\downarrow})^T$. In order to study topological properties, we perform a unitary transformation $\tilde{H}_{\text{BdG}}(\mathbf{k}) = U(\mathbf{k}) \hat{H}_{\text{BdG}}(\mathbf{k}) U(\mathbf{k})^\dagger$. By choosing $U(\mathbf{k}) = \begin{pmatrix} 1 & 0 \\ 0 & e^{ik\cdot\tau} \end{pmatrix} \sigma \otimes s_0 \otimes \tau_0$ and $\tau = (0, -\frac{1}{\sqrt{3}}, \frac{1}{2})$, $\tilde{H}_{\text{BdG}}(\mathbf{k})$ is periodic with respect to the translation $\mathbf{k} \rightarrow \mathbf{k} + \mathbf{K}$ with \mathbf{K} being a reciprocal lattice vector.

Weyl nodes are specified by a topological Weyl charge defined by a monopole of Berry flux, $q_i = \frac{1}{2\pi} \oint_S d\mathbf{k} \cdot \tilde{\mathbf{F}}(\mathbf{k})$, where the Berry flux,

$$F_i(\mathbf{k}) = -i \varepsilon^{ijk} \sum_{E_n(\mathbf{k}) < 0} \partial_{k_j} \langle u_n(\mathbf{k}) | \partial_{k_k} u_n(\mathbf{k}) \rangle, \quad (4)$$

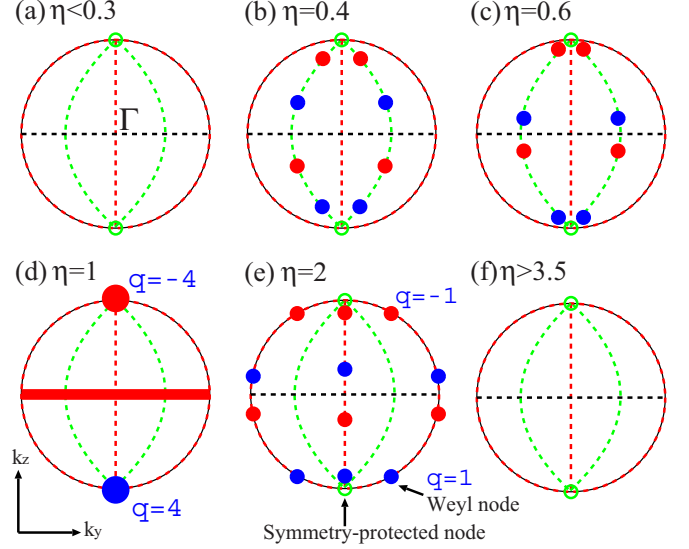


FIG. 2. Illustration of pair creation and annihilation of Weyl nodes on a Γ -FS. Projection from the k_x axis is shown. In (b), (c), and (e), blue and red closed circles show single Weyl nodes with $q_i = 1$ and -1 , respectively. Large circles in (d) are spin-degenerate double Weyl nodes with $q_i = \pm 4$. Thick solid line in (d) shows a quadratic line node at $k_z = 0$. Green open circles are trivial point nodes protected by symmetry. Dashed lines illustrate nodal lines in the purely f -wave states, although they disappear in a generic E_{2u} state.

is integrated on a closed surface surrounding an isolated point node. We identify Weyl nodes by calculating k_z -dependent Chern number,

$$\nu(k_z) = \frac{1}{2\pi} \int d\mathbf{k}_{\parallel} F_z(\mathbf{k}), \quad (5)$$

on a two-dimensional k_x - k_y plane [46–48]. A wave function and energy of Bogoliubov quasiparticles are denoted by $|u_n(\mathbf{k})\rangle$ and $E_n(\mathbf{k})$, respectively. A jump in the Chern number is equivalent to the sum of Weyl charges at k_z . That is, $\nu(k_z + 0) - \nu(k_z - 0) = \sum_i q_i$. Thus, counting symmetry-related point nodes and comparing it with a jump in $\nu(k_z)$, we are able to identify Weyl charges.

First, we elucidate Weyl nodes on the Γ -FS. This is a simple case, because only one of the bands crosses the Fermi level although the two-band model is adopted. The nodal structures are qualitatively the same as those in the single-band model which are analytically expressed in the Supplemental Material [49]. Then, the d -wave order parameter does not play any important role. On the other hand, the p - f mixing in the order parameter eliminates line nodes in the chiral f -wave state [11] in accordance with Blount's theorem [20, 21], except for $\eta = 1$. Diagonalizing $\tilde{H}_{\text{BdG}}(\mathbf{k})$, we obtain the superconducting gap illustrated in Fig. 2. Instead of line nodes, Weyl nodes (closed circles in Fig. 2) appear in the B-phase, in addition to the symmetry-protected point nodes at the poles on the FS. The former is identified as Weyl nodes by Fig. 3(a). The Chern number jumps by ± 4 , and we find four point nodes at a certain k_z . Thus the point nodes are identified as single Weyl nodes with a unit charge $q_i = \pm 1$. In total, eight pairs of single Weyl nodes are produced. Since the spin degeneracy

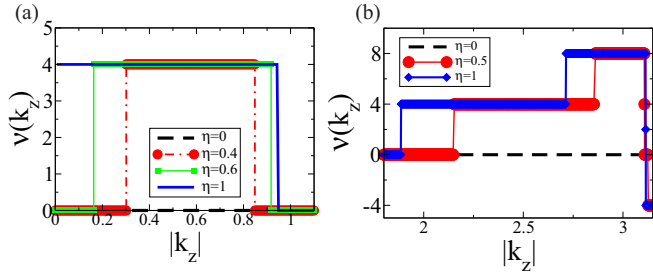


FIG. 3. Chern number of the two-dimensional BdG Hamiltonian parametrized by k_z for (a) a Γ -FS reproduced by the parameter set $(t, t_z, t', \alpha, \mu, \Delta, \delta) = (1, 4, 1, 0, 16, 0.4, 0.01)$ and for (b) A-FSs by $(1, -4, 1, 0, 12, 0.1, 0.04)$.

is lifted owing to the nonunitary order parameter, the spinless single Weyl nodes are realized even at zero magnetic field.

Here we show pair creation, annihilation, and coalescence of Weyl nodes. Because the particle-hole symmetry is implemented in the BdG Hamiltonian for superconductors, the time-reversal symmetry ensures the chiral symmetry prohibiting Weyl nodes [50]. Therefore, the A- and C-phases do not host Weyl nodes as illustrated in Figs. 2(a) and 2(f). The triviality is robust against a weak time reversal symmetry breaking because the gap closing is required for the topological transition. Therefore, pair creation of Weyl nodes does not occur at the thermodynamical A-B and B-C phase boundaries, but occurs in the B-phase. For the parameters in Fig. 3(a), we see the pair creation at $\eta = 0.3$ and 3.5. Accordingly, the Weyl superconducting phase is illustrated in Fig. 1(a).

When the parameter η is increased from zero by decreasing the magnetic field or increasing the temperature, the Weyl nodes emerge and move along nodal lines of the $f_{(x^2-y^2)z}$ -wave component [Figs. 2(b) and 2(c)]. At $\eta = 1$, four pairs of Weyl nodes cause pair annihilation at $k_z = 0$, and the remaining eight Weyl nodes coalesce into a pair of spin-degenerate double Weyl nodes ($q_i = \pm 4$) at the poles [Fig. 2(d)]. When η increases from unity, eight pairs of Weyl nodes again appear on nodal lines of the f_{xyz} -wave component [Fig. 2(e)]. These pair creation, pair annihilation, and coalescence of Weyl nodes occur in the generic E_{2u} state as a result of the p - f mixing [49], although the chiral f -wave state hosts only Weyl nodes at the poles which are shown in Fig. 2(d) [34].

The pair annihilation and coalescence of Weyl nodes give rise to unusual gap structure at $\eta = 1$. Since the B-phase is weakly nonunitary due to small δ , two nonequivalent superconducting gaps $\Delta_{\pm}(\mathbf{k})$ are obtained [10]. We see an intriguing nodal structure in the small gap $\Delta_{-}(\mathbf{k})$. The pair annihilation leads to *quadratic line node* at $k_z = 0$, that is, $\Delta_{-}(\mathbf{k}) \propto |k_z|^2$, which is distinct from a usual linear line node with $\Delta(\mathbf{k}) \propto |k_z|$ and gives rise to a low-energy DOS, $\rho(\omega) \propto \sqrt{\omega}$. On the other hand, the coalescence of Weyl nodes results in *cubic point nodes*, $\Delta_{-}(\mathbf{k}) \propto |k_{\parallel}|^3$, at the poles.

Next, we investigate the A-FSs. This is an intriguing case, because the nonsymmorphic crystal symmetry causes gap nodes. The intersublattice hybridization $a(\mathbf{k})$ vanishes at $k_z = \pi$, and resulting sublattice degeneracy leads to paired FSs, as shown in Fig. 5(a). Although the degeneracy is partly lifted by the SOC, the symmetry protects the degeneracy along

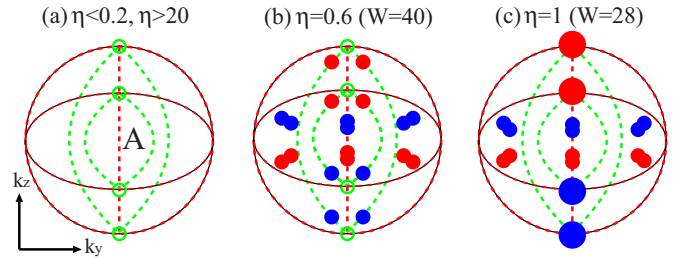


FIG. 4. Illustration of Weyl nodes on the A-FSs drawn by numerically diagonalizing the BdG Hamiltonian for the parameter set in Fig. 3(b). Thin solid lines show paired FSs. Other marks are the same as Fig. 2. We show the number of Weyl nodes W .

$k_{\parallel} \parallel [010]$ and symmetric lines (A-L lines) [51]. Thus any single band model breaks down, and our two-band model is a minimal model.

Figure 3(b) shows an increase in the Chern number $\nu(k_z) = 0 \rightarrow 4 \rightarrow 8$ with $|k_z|$, indicating eight pairs of single Weyl nodes. These Weyl nodes arise from the p - f mixing as we clarified for the Γ -FS. The Chern number $\nu(k_z) = 8$ is obtained just by the multiplication 2 due to the two bands. When we furthermore increase $|k_z|$ to π , interestingly the Chern number changes to -4 given by the d -wave component of the order parameter. Since the sublattice-singlet d -wave component induces interband pairing, it is negligible in most regions of the Brillouin zone. However, the interband pairing may play an important role around $k_z = \pi$ where the two bands are nearly degenerate. The jump of Chern number, $\nu(k_z) = 8 \rightarrow -4$, results in twelve pairs of single Weyl nodes. Twenty pairs of Weyl nodes appear on the A-FSs in total [Fig. 4(b)]. In contrast to eight pairs due to the p - f mixing, the twelve pairs of Weyl nodes arising from the d - f mixing in the order parameter are robust in the sixfold rotation-symmetric state at $\eta = 1$ [Fig. 4(c)], because twelve is a multiple of six.

Now we show a gap node induced by the SOC. The nonsymmorphic space group allows a line node at the Brillouin zone face as pointed out by Norman [52] as a counterexample of Blount's theorem. Contrary to Norman's argument, we obtain a *nodal arc* on the FSs. That is, a part of FS is gapped as shown in Fig. 5. Seemingly contradictory results are obtained because we plot the excitation gap near the FSs,

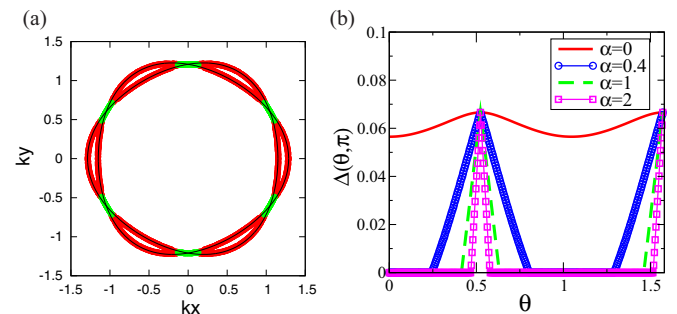


FIG. 5. (a) A-FSs at the Brillouin zone face, $k_z = \pm\pi$. Gapless and gapped regions at $\alpha = 1$ are shown by red and green lines, respectively. (b) Angle dependence of the gap $\Delta(\theta, \pi)$ for various SOC parameters. The other parameters are the same as Fig. 3(b).

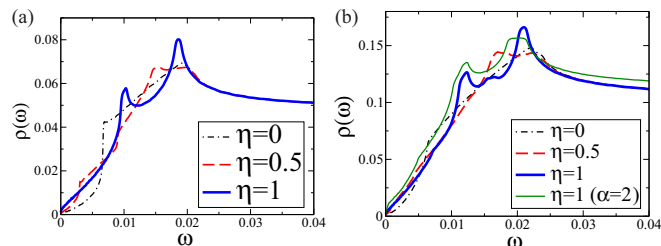


FIG. 6. DOS of (a) a Γ -FS and (b) A-FSs. Parameters are the same as Fig. 3. We also show a result for $\alpha = 2$ in (b) by the thin green solid line in order to clarify the contribution of the SOC-induced arc node.

$\Delta(\theta, \pi) = \min_{k,n} |E_n(k \cos \theta, k \sin \theta, \pi)|$, although Norman's argument revealed the disappearance of intraband Cooper pairs. The excitation spectrum is actually gapped around $k_{\parallel} \parallel [010]$ owing to the interband Cooper pairing.

Finally, we show the DOS in Fig. 6. Even though the line node is absent in accordance with Blount's theorem, the DOS shows a linear energy dependence in the B-phase in agreement with experimental observations [11,12]. Although the SOC-induced arc node on the A-FSs [52] increases the DOS around $\omega = 0$, its contribution is not dominant, as shown in Fig. 6(b). Thus it is indicated that at most 44 point nodes on paired A-FSs and 54 point nodes on three Γ -FSs give rise to line-node-like behaviors. The thermal conductivity measurement has been a powerful tool in identifying the superconducting symmetry of UPt_3 [12,19]. The saturating ratio κ_c/κ_b supporting the chiral f -wave state [12,53,54] also supports the generic E_{2u} state which has point nodes on general points of Brillouin zone. A residual thermal conductivity much smaller than the universal value of line nodal superconductors [55] may be consistent with point nodal E_{2u} state. Nearly isotropic ab -plane field-angle dependence [19,56] may be explained by the cancellation of anisotropy from nearly 100 point nodes.

A square-root dependence $\rho(\omega) \propto \sqrt{\omega}$ is obtained in the low-energy region at $\eta = 1$ [Fig. 6(a)] as a result of the

quadratic line node. However, unusual $\sqrt{\omega}$ dependence may be obscured by the vortex scattering since $\eta = 1$ is not realized at zero magnetic field as illustrated in Fig. 1(a) [43].

Conclusion. To conclude, the E_{2u} -pairing state in nonsymmorphic UPt_3 is a Weyl superconducting state which shows the pair creation, pair annihilation, and coalescence of Weyl nodes. The $p + d + f$ mixing in the order parameter partly due to the nonsymmorphic crystal symmetry causes these unusual behaviors which have not been observed in a chiral f -wave state [34]. The topologically distinct properties give rise to Majorana arcs in surface states analogous to the recently observed Fermi arc [27–29], resulting in a zero-field thermal Hall conductivity [33,34] and quasiparticle interference [57]. Tunable positions of Weyl nodes by temperature and magnetic field may enable experimental observations and also may induce the chiral anomaly through a topological defect in the combined real and momentum space [58].

Our results are compatible with Blount's theorem [20,21], but at most 98 point nodes and the SOC-induced arc node lead to line node behaviors in the DOS, consistent with experimental observations in UPt_3 [12]. A generic E_{2u} -pairing state studied here may also be consistent with experiments incompatible with the chiral f -wave state [13,19,55,56], although further theoretical developments taking account of multigap structure are desired.

Nonsymmorphic symmetry may be weakly broken either by a crystal distortion [59] or by an antiferromagnetic order in UPt_3 [44,45]. Even in this case, the topologically protected Weyl nodes are robust, although the symmetry-protected SOC-induced arc node is gapped.

Acknowledgments. The authors are grateful to K. Izawa, H. Harima, S. Kobayashi, T. Nomoto, M. Sato, and K. Shiozaki for fruitful discussions. This work was supported by the "Topological Quantum Phenomena" (Grant No. JP25103711) and "J-Physics" (Grant No. JP15H05884) Grant-in Aid for Scientific Research on Innovative Areas from MEXT of Japan, and by JSPS KAKENHI Grants No. JP24740230, No. JP15K05164, No. JP15H05745, and No. JP16H00991.

-
- [1] C. L. Kane and E. J. Mele, Quantum Spin Hall Effect in Graphene, *Phys. Rev. Lett.* **95**, 226801 (2005).
 - [2] A. P. Schnyder, S. Ryu, A. Furusaki, and A. W. Ludwig, Classification of topological insulators and superconductors in three spatial dimensions, *Phys. Rev. B* **78**, 195125 (2008).
 - [3] A. Kitaev, in *Periodic Table for Topological Insulators and Superconductors*, AIP Conf. Proc. No. 1134 (AIP, New York, 2009), p. 22.
 - [4] X.-L. Qi and S.-C. Zhang, Topological insulators and superconductors, *Rev. Mod. Phys.* **83**, 1057 (2011).
 - [5] Y. Yanase, T. Jujo, T. Nomura, H. Ikeda, T. Hotta, and K. Yamada, Theory of superconductivity in strongly correlated electron systems, *Phys. Rep.* **387**, 1 (2003).
 - [6] G. R. Stewart, Z. Fisk, J. O. Willis, and J. L. Smith, Possibility of Coexistence of Bulk Superconductivity and Spin Fluctuations in UPt_3 , *Phys. Rev. Lett.* **52**, 679 (1984).
 - [7] R. A. Fisher, S. Kim, B. F. Woodfield, N. E. Phillips, L. Taillefer, K. Hasselbach, J. Flouquet, A. L. Giorgi, and J. L. Smith, Specific Heat of UPt_3 : Evidence for Unconventional Superconductivity, *Phys. Rev. Lett.* **62**, 1411 (1989).
 - [8] G. Bruls, D. Weber, B. Wolf, P. Thalmeier, B. Luthi, A. de Visser, and A. Menovsky, Strain-order-parameter Coupling and Phase Diagrams in Superconducting UPt_3 , *Phys. Rev. Lett.* **65**, 2294 (1990).
 - [9] S. Adenwalla, S. W. Lin, Q. Z. Ran, Z. Zhao, J. B. Ketterson, J. A. Sauls, L. Taillefer, D. G. Hinks, M. Levy, and B. K. Sarma, Phase Diagram of UPt_3 from Ultrasonic Velocity Measurements, *Phys. Rev. Lett.* **65**, 2298 (1990).
 - [10] M. Sigrist and K. Ueda, Phenomenological theory of unconventional superconductivity, *Rev. Mod. Phys.* **63**, 239 (1991).
 - [11] J. A. Sauls, The order parameter for the superconducting phases of UPt_3 , *Adv. Phys.* **43**, 113 (1994).

- [12] R. Joynt and L. Taillefer, The superconducting phases of UPt₃, *Rev. Mod. Phys.* **74**, 235 (2002).
- [13] H. Tou, Y. Kitaoka, K. Ishida, K. Asayama, N. Kimura, Y. Onuki, E. Yamamoto, Y. Haga, and K. Maezawa, Nonunitary Spin-triplet Superconductivity in UPt₃: Evidence from ¹⁹⁵Pt Knight Shift Study, *Phys. Rev. Lett.* **80**, 3129 (1998).
- [14] A. Y. Kitaev, Unpaired Majorana fermions in quantum wires, *Phys. Usp.* **44**, 131 (2001).
- [15] M. Sato, Topological odd-parity superconductors, *Phys. Rev. B* **81**, 220504 (2010).
- [16] Y. Tanaka, M. Sato, and N. Nagaosa, Symmetry and topology in superconductors odd-frequency pairing and edge states, *J. Phys. Soc. Jpn.* **81**, 011013 (2012).
- [17] E. R. Schemm, W. J. Gannon, C. M. Wishne, W. P. Halperin, and A. Kapitulnik, Observation of broken time-reversal symmetry in the heavy-fermion superconductor UPt₃, *Science* **345**, 190 (2014).
- [18] J. D. Strand, D. J. Bahr, D. J. Van Harlingen, J. P. Davis, W. J. Gannon, and W. P. Halperin, The transition between real and complex superconducting order parameter phases in UPt₃, *Science* **328**, 1368 (2010).
- [19] Y. Machida, A. Itoh, Y. So, K. Izawa, Y. Haga, E. Yamamoto, N. Kimura, Y. Onuki, Y. Tsutsumi, and K. Machida, Twofold Spontaneous Symmetry Breaking in the Heavy-fermion Superconductor UPt₃, *Phys. Rev. Lett.* **108**, 157002 (2012); K. Izawa, Y. Machida, A. Itoh, Y. So, K. Ota, Y. Haga, E. Yamamoto, N. Kimura, Y. Onuki, Y. Tsutsumi, and K. Machida, Pairing symmetry of UPt₃ probed by thermal transport tensors, *J. Phys. Soc. Jpn.* **83**, 061013 (2014).
- [20] E. I. Blount, Symmetry properties of triplet superconductors, *Phys. Rev. B* **32**, 2935 (1985).
- [21] S. Kobayashi, K. Shiozaki, Y. Tanaka, and M. Sato, Topological Blount's theorem of odd-parity superconductors, *Phys. Rev. B* **90**, 024516 (2014).
- [22] A line node protected by a nonsymmorphic space group symmetry has been proposed [52] as a counterexample of Blount's theorem. Indeed, our model shows an arc node protected by the screw and glide symmetry of UPt₃. On the other hand, the line node in the chiral *f*-wave state is not protected by the nonsymmorphic symmetries.
- [23] T. Meng and L. Balents, Weyl superconductors, *Phys. Rev. B* **86**, 054504 (2012).
- [24] S. Murakami, Phase transition between the quantum spin Hall and insulator phases in 3D: emergence of a topological gapless phase, *New J. Phys.* **9**, 356 (2007).
- [25] X. Wan, A. M. Turner, A. Vishwanath, and S. Y. Savrasov, Topological semimetal and Fermi-arc surface states in the electronic structure of pyrochlore Iridates, *Phys. Rev. B* **83**, 205101 (2011).
- [26] A. A. Burkov and L. Balents, Weyl Semimetal in a Topological Insulator Multilayer, *Phys. Rev. Lett.* **107**, 127205 (2011).
- [27] S.-Y. Xu, I. Belopolski, N. Alidoust, M. Neupane, C. Zhang, R. Sankar, S.-M. Huang, C.-C. Lee, G. Chang, B. Wang, G. Bian, H. Zheng, D. S. Sanchez, F. Chou, H. Lin, S. Jia, and M. Z. Hasan, Discovery of a Weyl fermion semimetal and topological Fermi arcs, *Science* **349**, 613 (2015).
- [28] B. Q. Lv, N. Xu, H. M. Weng, J. Z. Ma, P. Richard, X. C. Huang, L. X. Zhao, G. F. Chen, C. E. Matt, F. Bisti, V. N. Strocov, J. Mesot, Z. Fang, X. Dai, T. Qian, M. Shi, and H. Ding, Observation of Weyl nodes in TaAs, *Nat. Phys.* **11**, 724 (2015).
- [29] L. X. Yang, Z. K. Liu, Y. Sun, H. Peng, H. F. Yang, T. Zhang, B. Zhou, Y. Zhang, Y. F. Guo, M. Rahn, D. Prabhakaran, Z. Hussain, S.-K. Mo, C. Felser, B. Yan, and Y. L. Chen, Weyl semimetal phase in the non-centrosymmetric compound TaAs, *Nat. Phys.* **11**, 728 (2015).
- [30] X. Huang, L. Zhao, Y. Long, P. Wang, D. Chen, Z. Yang, H. Liang, M. Xue, H. Weng, Z. Fang, X. Dai, and G. Chen, Observation of the Chiral-anomaly-induced Negative Magnetoresistance in 3D Weyl Semimetal TaAs, *Phys. Rev. X* **5**, 031023 (2015).
- [31] G. E. Volovik, Flat band in the core of topological defects: bulk-vortex correspondence in topological superfluids with Fermi points, *JETP Lett.* **93**, 66 (2011).
- [32] J. D. Sau and S. Tewari, Topologically protected surface Majorana arcs and bulk Weyl fermions in ferromagnetic superconductors, *Phys. Rev. B* **86**, 104509 (2012).
- [33] M. H. Fischer, T. Neupert, C. Platt, A. P. Schnyder, W. Hanke, J. Goryo, R. Thomale, and M. Sigrist, Chiral *d*-wave superconductivity in SrPtAs, *Phys. Rev. B* **89**, 020509 (2014).
- [34] P. Goswami and A. H. Nevidomskyy, Topological Weyl superconductor to diffusive thermal Hall metal crossover in the B phase of UPt₃, *Phys. Rev. B* **92**, 214504 (2015).
- [35] Y. Saito, Y. Nakamura, M. S. Bahramy, Y. Kohama, J. Ye, Y. Kasahara, Y. Nakagawa, M. Onga, M. Tokunaga, T. Nojima, Y. Yanase, and Y. Iwasa, Superconductivity protected by spin-valley locking in gate-tuned MoS₂, *Nat. Phys.* **12**, 144 (2016).
- [36] M. H. Fischer, F. Loder, and M. Sigrist, Superconductivity and local noncentrosymmetry in crystal lattices, *Phys. Rev. B* **84**, 184533 (2011).
- [37] D. Maruyama, M. Sigrist, and Y. Yanase, Locally non-centrosymmetric superconductivity in multilayer systems, *J. Phys. Soc. Jpn.* **81**, 034702 (2012).
- [38] L. Taillefer and G. G. Lonzarich, Heavy-fermion Quasiparticles in UPt₃, *Phys. Rev. Lett.* **60**, 1570 (1988); M. R. Norman, R. C. Albers, A. M. Boring, and N. E. Christensen, Fermi surface and effective masses for the heavy-electron superconductors UPt₃, *Solid State Commun.* **68**, 245 (1988).
- [39] N. Kimura, R. Settai, Y. Onuki, H. Toshima, E. Yamamoto, K. Maezawa, H. Aoki, and H. Harima, Magnetoresistance and de Haas-van Alphen effect in UPt₃, *J. Phys. Soc. Jpn.* **64**, 3881 (1995).
- [40] G. J. McMullan, P. M. C. Rourke, M. R. Norman, A. D. Huxley, N. Doiron-Leyraud, J. Flouquet, G. G. Lonzarich, A. McCollam, and S. R. Julian, The Fermi surface and *f*-valence electron count of UPt₃, *New J. Phys.* **10**, 053029 (2008).
- [41] T. Nomoto and H. Ikeda, Exotic multi-gap structure in UPt₃ unveiled by the first-principles analysis, [arXiv:1607.02708](https://arxiv.org/abs/1607.02708).
- [42] See Supplemental Material at <http://link.aps.org/supplemental/10.1103/PhysRevB.94.174502> for a theoretical derivation of order parameter in a generic E_{2u} state.
- [43] See Supplemental Material at <http://link.aps.org/supplemental/10.1103/PhysRevB.94.174502>. The range of the parameter η is listed in S3 (Table S2). The temperature and magnetic field dependence of the parameter η is explained in details on the basis of the Ginzburg-Landau theory.
- [44] G. Aeppli, E. Bucher, C. Broholm, J. K. Kjems, J. Baumann, and J. Hufnagl, Magnetic Order and Fluctuations in Superconducting UPt₃, *Phys. Rev. Lett.* **60**, 615 (1988).

- [45] S. M. Hayden, L. Taillefer, C. Vettier, and J. Flouquet, Antiferromagnetic order in UPt_3 under pressure: Evidence for a direct coupling to superconductivity, *Phys. Rev. B* **46**, 8675(R) (1992).
- [46] D. J. Thouless, M. Kohmoto, M. P. Nightingale, and M. den Nijs, Quantized Hall Conductance in a Two-Dimensional Periodic Potential, *Phys. Rev. Lett.* **49**, 405 (1982).
- [47] M. Kohmoto, Topological invariant and the quantization of the Hall conductance, *Ann. Phys. (NY)* **160**, 343 (1985).
- [48] T. Fukui, Y. Hatsugai, and H. Suzuki, Chern numbers in discretized Brillouin zone: efficient method of computing (spin) Hall conductances, *J. Phys. Soc. Jpn.* **74**, 1674 (2005).
- [49] See Supplemental Material at <http://link.aps.org/supplemental/10.1103/PhysRevB.94.174502> for analytic results of nodal structure in the single band model.
- [50] In the presence of the time-reversal symmetry, the BdG Hamiltonian on a generic two-dimensional momentum space belongs to the symmetry class AIII [2,3]. Then, the Chern number on a closed surface must be zero.
- [51] The degeneracy of two bands at $k_z = \pi$ and $\mathbf{k}_{\parallel} \parallel [010]$ (A - L lines) is protected by the crystal symmetry. This is proved by using the relations, $\{IG_{xz}, IT\} = 0$, $\{IG_{xz}, M_{yz}\} = 0$, and $(IG_{xz})^2 = -1$, at $k_z = \pm\pi$. Inversion symmetry, time-reversal symmetry, and mirror symmetry are represented by $I = \sigma_x$, $T = is_y K$, and $M_{yz} = is_x$, respectively. The glide symmetry is represented by $G_{xz} = s_y \sigma_y$ at $k_z = \pm\pi$ while $G_{xz} = is_y \sigma_x$ at $k_z = 0$. We will show details elsewhere.
- [52] M. R. Norman, Odd parity and line nodes in heavy-fermion superconductors, *Phys. Rev. B* **52**, 15093 (1995); T. Micklitz and M. R. Norman, Odd parity and line nodes in nonsymmorphic superconductors, *ibid.* **80**, 100506(R) (2009).
- [53] B. Lussier, B. Ellman, and L. Taillefer, Determination of the gap structure in UPt_3 by thermal conductivity, *Phys. Rev. B* **53**, 5145 (1996).
- [54] M. R. Norman and P. J. Hirschfeld, Heat transport and the nature of the order parameter in superconducting UPt_3 , *Phys. Rev. B* **53**, 5706 (1996).
- [55] H. Suderow, J. P. Brison, A. D. Huxley, and J. Flouquet, Thermal conductivity and gap structure of the superconducting phases of UPt_3 , *J. Low Temp. Phys.* **108**, 11 (1997).
- [56] S. Kittaka, K. An, T. Sakakibara, Y. Haga, E. Yamamoto, N. Kimura, Y. Onuki, and K. Machida, Anomalous field-angle dependence of the specific heat of heavy-fermion superconductor UPt_3 , *J. Phys. Soc. Jpn.* **82**, 024707 (2013).
- [57] S. Kourtis, J. Li, Z. Wang, A. Yazdani, and B. A. Bernevig, Universal signatures of Fermi arcs in quasiparticle interference on the surface of Weyl semimetals, *Phys. Rev. B* **93**, 041109(R) (2016).
- [58] G. E. Volovik, Topology of chiral superfluid: Skyrmions, Weyl fermions and chiral anomaly, *JETP Lett.* **103**, 140 (2016).
- [59] D. A. Walko, J.-I. Hong, T. V. Chandrasekhar Rao, Z. Wawrzak, D. N. Seidman, W. P. Halperin, and M. J. Bedzyk, Crystal structure assignment for the heavy-fermion superconductor UPt_3 , *Phys. Rev. B* **63**, 054522 (2001).